Increasing Intensity of Extreme Heatwaves: The Crucial Role of Metrics

Emmanuele Russo[1] [ID] and Daniela I. V. Domeisen[1,2] [ID]

[1]Institute for Atmospheric and Climate Science, ETH Zurich, Zürich, Switzerland, [2]Université de Lausanne, Lausanne, Switzerland

Abstract In weather and climate applications, a wide range of commonly employed heatwave intensity indices relies either on cumulative or averaged values of temperature-based variables. In this study, by comparing four different heatwave intensity indices applied to reanalysis data we show that metrics based on cumulative or averaged values lead to important differences in the detection of the most intense events of the period 1950–2021. This suggests that particular attention is needed when using the two families of metrics for assessing heatwave intensity. Indices based on cumulative values should be preferred over the ones relying on temporal averages, better allowing for the comparison of events of different length. Under these considerations, one of the considered cumulative indices is used for characterizing heatwaves of the period 1950–2021, showing that heatwaves that were unlikely before 1986 have become almost 10 times more frequent and up to three times more intense during recent times.

Plain Language Summary Heatwave intensity represents a measure of how extreme an event is, which is directly connected to the severity of its impact on the population and natural ecosystems. In weather and climate applications, a wide range of heatwave intensity indices exists that are used. In this work we show that two families of commonly employed indices for heatwave intensity, either relying on cumulative or averaged values of temperature-based variables, lead to important differences in the detection of the most intense events occurring globally over the period 1950–2021. This suggests that extreme care is needed in the use of the two families of metrics for the assessment of heatwave intensity. Indices based on cumulative values represent a more appropriate choice than the ones relying on temporal averages, since they better allow for the comparison of events of different length. Additionally, using one of the considered cumulative metrics for heatwave intensity, we investigate the trends of very extreme events over the period 1950–2021. The results show that for all the considered regions, heatwaves that were rarely recorded during 1950–1985 have become up to 10 times more likely and up to three times more intense over 1986–2021.

1. Introduction

Heatwaves are defined as extended periods of excessive heat (Perkins & Alexander, 2013; Perkins-Kirkpatrick & Lewis, 2020). They are considered to be one of the most harmful natural hazards, with serious implications for human health (Cusack et al., 2011; Fischer & Schär, 2010; Gasparrini et al., 2015; Kjellstrom et al., 2013; Kovats & Kristie, 2006; López-Bueno et al., 2021; Williams et al., 2012), infrastructure (Forzieri et al., 2018; Maggiotto et al., 2021; Stone Jr et al., 2021), the economy (García-León et al., 2021; Xia et al., 2018) and natural ecosystems (Breshears et al., 2021; Siegle et al., 2018). In the climate science community heatwaves are characterized through measures of their intensity, maximum amplitude, duration, frequency and spatial extent (Domeisen et al., 2022; Perkins-Kirkpatrick & Lewis, 2020). There exists a plethora of different metrics for characterizing each of these features, often tailored to the specific needs of a given study, depending on the sector and area of the application. This heterogeneity in the use of metrics does not always allow for a comprehensive understanding of how heatwaves differ over time as well as by region (Perkins & Alexander, 2013; Perkins-Kirkpatrick & Lewis, 2020; Russo & Sterl, 2011; Russo et al., 2015).

This is particularly true in the case of heatwave intensity, a relevant feature directly linked to the severity of impacts on natural ecosystems (Iwasaki & Noda, 2018). According to the definition proposed by Biondi et al. (2005, 2008) and Zuniga et al. (2021) for hydro-climatic extreme events exceeding the value of a given threshold, the intensity or magnitude of a heatwave is given by the cumulative value of total exceedances of the threshold over the consecutive days of the event. While several climate studies use this definition applied to

Writing – review & editing: Emmanuele Russo, Daniela I. V. Domeisen

daily temperatures (Russo & Sterl, 2011; Russo et al., 2014, 2015, 2016), there are many cases where the terms intensity or magnitude of a heatwave are instead used for referring to averaged values of temperature-based variables (Bitencourt et al., 2016; Cowan et al., 2014; Cueto et al., 2010; Ganguly et al., 2009; Holbrook et al., 2022; Lhotka & Kyselỳ, 2015; Perkins et al., 2012; Schaeffer & Roughan, 2017; Ward et al., 2016; Yu et al., 2020; Zhang et al., 2020). Despite their extensive use for characterizing the same heatwave feature, the two definitions are not equivalent and they might lead to different conclusions. There is indeed the need to better assess the effects of the use of metrics for heatwave intensity based on these two different definitions, highlighting possible drawbacks and contributing to a more unified and consistent application of indices in climate studies. This will further allow for a better comparability of events over time and in space. Driven by this goal, in this study the most intense heatwaves occurring over the period 1950–2021 are detected and characterized at a global scale by means of four different heatwave intensity indices either based on cumulative or averaged values of temperature-based variables.

All of the presented analyses are conducted on the ERA5-Land reanalysis data set (Muñoz-Sabater et al., 2021). Prior to the indices calculation, ERA5-Land is evaluated against the Berkeley-Earth and JRA-55 data sets to identify areas where ERA5-Land can be considered more reliable in terms of interannual variability of daily maximum temperatures. Then, the most intense heatwaves and the year in which these events occur over the period from 1950 to 2021, according to ERA5-Land, are determined using the four considered indices, with the goal of highlighting different conclusions arising from different methods. Finally, in a last step, differences between the first and the second half of the considered study period in terms of occurrence and magnitude of very extreme heatwaves are investigated for one of the proposed metrics and specific regions.

2. Methods

2.1. Data

The analyses presented in this study are based on daily maximum temperature for the period 1950–2021 from the ERA5-Land reanalysis data set, interpolated through conservative remapping on a regular grid at a spatial resolution of 0.25°longitude × 0.25°latitude.

ERA5-Land provides hourly information of surface variables at a spatial resolution of ∼9 km. The data is derived from a single simulation with the European Centre for Medium-Range Weather Forecasts *Carbon Hydrology-Tiles scheme for Surface Exchanges over Land* model, forced by meteorological fields of the lowest atmospheric level of the ERA5 reanalysis (Hersbach et al., 2020), with an additional lapse-rate correction (Muñoz-Sabater et al., 2021). The model version employed for the production of ERA5-Land is very similar to the one used for ERA5, but with an updated parameterization of the soil thermal conductivity after Peters-Lidard et al. (1998), technical fixes improving the conservation of soil moisture balance and additional improvements for the calculation of potential evapotranspiration fluxes. These improvements do not lead to remarkable differences between ERA5-Land and ERA5, given the fact that they still share common and similar parameterizations of land processes (Muñoz-Sabater et al., 2021). The main added value of ERA5-Land over ERA5 is attributable, according to Muñoz-Sabater et al. (2021), to the non-linear dynamical downscaling with corrected thermodynamic input, allowing for example, to better discriminate between land and sea points over coastal areas.

The reliability of ERA5-Land in terms of the interannual variability of the seasonal maxima of daily maximum temperatures is assessed here against two additional data sets: the gridded Berkeley-Earth observational data set (Rohde et al., 2013) (BE hereafter) and the Japanese reanalysis JRA-55 (Kobayashi et al., 2015). These data sets are chosen as they have a temporal coverage similar to ERA5-Land, with BE starting in 1950 and JRA-55 in 1958. The BE data set provides daily values of maximum temperature on a regular grid with a spatial resolution of 1°longitude × 1°latitude. These values are originally derived from observations with sub-hourly to hourly temporal resolution (Rohde et al., 2013). On the other hand, JRA-55 daily maximum temperatures are calculated here from the original 6-hourly gridded data presenting a spatial resolution of 1.25°longitude × 1.25°latitude. For the comparison against these two other data sets, ERA5-Land is first upscaled onto the respective coarser-resolution grids from each data set, through conservative remapping. Additionally, daily maxima of ERA5-Land derived from 1-hourly and 6-hourly data are respectively used for the comparison against BE and JRA-55.

All the employed data sets cover the entire globe. However, in this study only the data between −80° and 80°N are considered.

2.2. Heatwave Definition

Heatwaves are generally defined as consecutive periods with extreme temperatures exceeding a given threshold (Data, 2009; Domeisen et al., 2022). Similarly to Russo et al. (2015) and Perkins-Kirkpatrick and Lewis (2020), here we consider heatwaves as events of at least 3 consecutive days with temperatures exceeding the threshold $Tr90_d$, calculated as the 90th percentile of daily maximum temperatures in a sliding window of 30 days around the considered day d, over a 30-year reference period. We select the period from 1961 to 1990 as our reference period, as this period is often considered as a reference for long-term climate change assessments (Tavakol et al., 2020) and as the employed data sets start on 1958 at the latest.

We separately analyze heatwaves in different seasons. In order to include heatwaves that start in a season and finish in another, periods of 5 months are selected around each 3-month season for the definition of heatwaves, with an additional month at the beginning and at the end of their classical definition (e.g., May–September for boreal summer). Then, to avoid counting single events twice, heatwaves are assigned to a specific season depending on the largest number of days they have in the three central months of each season.

2.3. Heatwave Intensity Indices

With the goal of identifying possible differences arising from different definitions of heatwave intensity extensively applied in weather and climate applications, four indices are considered in this study, either using accumulated or averaged values of temperature-based variables. The first of these indices is based on the magnitude assessment of single heatwave events, while the other three jointly consider all the days characterized by a heatwave during an entire season. Below, the four considered indices are described in detail.

2.3.1. HWMId

The HeatWave Magnitude Index daily (HWMId) of Russo et al. (2015) is calculated here as the sum of the daily magnitude index M_d over each of the days n composing a single heatwave event hw:

$$HWMId_{hw} = \sum_{d=1}^{n_{hw}} M_d(T_d) \tag{1}$$

where T_d is the daily maximum temperature on day d of the heatwave hw. For computing M_d, first anomalies of daily maximum temperature are computed for the day d with respect to the 25th percentile of seasonal temperature maxima over the reference period. Then, the anomalies are standardized by the interquartile range of the same seasonal temperature maxima over the reference period, allowing for a comparison of different points in space characterized by a different interannual variability of seasonal temperature maxima:

$$M_d(T_d) = \begin{cases} \dfrac{T_d - T_{30y25p}}{T_{30y75p} - T_{30y25p}} & if\ T_d > T_{30y25p} \\ 0 & if\ T_d \leq T_{30y25p} \end{cases} \tag{2}$$

T_{30y25p} and T_{30y75p} are, respectively, the 25th and 75th percentile values of the time-series composed of seasonal temperature maxima for the reference period 1961–1990 and considered season.

The methodology introduced by Russo et al. (2015) was designed for characterizing heatwaves over Europe, where the yearly temperature maxima generally occur in boreal summer. Here, considering almost the entire globe, it is important to acknowledge that over other areas yearly temperature maxima might take place at different times of the year. For this reason, similarly to Russo et al. (2016), the presented analyses are conducted separately for each season of the year (e.g., June July August (JJA)) and seasonal maxima of daily maximum temperatures are used in each case instead of the yearly maxima. Importantly, in this case a heatwave occurring between two distinct seasons would yield different HWMId values depending on the season it is attributed to. Hence, it becomes critically important to assign events unambiguously to individual seasons in order to ensure consistent analysis and interpretation.

2.3.2. HEATcum

The cumulative heat (HEATcum) defined in Perkins-Kirkpatrick and Lewis (2020), is given by the sum of the anomalies with respect to the threshold $Tr90_d$ in daily maximum temperatures (see Section 2.2), over all days characterized by a heatwave in a given season, for each of the years of the study period:

$$HEATcum = \sum_{d=1}^{n}(T_d - Tr90_d) \tag{3}$$

where d is the considered heatwave day and n the total number of heatwave days in the given season.

2.3.3. AVI

The heatwave Average Intensity (AVI) of Perkins-Kirkpatrick and Lewis (2020) is the average daily maximum temperature calculated over all the heatwave days of a season, for each year of the considered period:

$$AVI = \frac{\sum_{d=1}^{n} T_d}{n} \tag{4}$$

where, similarly to Equation 3, d is the day of a heatwave in the considered season, and n the total number of heatwave days in that season.

2.3.4. AVA

The heatwave Average Anomalies (here referred to as AVA) index is derived from the study of Perkins-Kirkpatrick and Lewis (2020) and represents the average of the daily maximum temperature anomalies with respect to the corresponding threshold $Tr90_d$, calculated for each year of the study period, over all the heatwave days of a given season:

$$AVA = \frac{\sum_{d=1}^{n}(T_d - Tr90_d)}{n} \tag{5}$$

where, again, d is the given heatwave day and n_{y_s} the total number of heatwave days in the considered season of a given year.

2.4. Changes in Very Extreme Events

In a last part of the study we conduct a comparison of the number and intensity of very extreme heatwaves between two periods of 36 years (hereafter referred to as Early Period (EP) and Late Period (LP), respectively), the first starting in 1950 and the second in 1986. Since for DJF it is only possible to compute 71 seasonal statistics over the period of ERA5-Land availability (1950–2021), in this case two periods of 35 years each are considered, starting in 1952 and 1987, respectively.

The comparison between the two periods is conducted separately for each season, for selected subregions of the Northern Hemisphere, namely Central North America (CNA), Europe (EUR) and Northern Asia (NAS, see Figure S1 in Supporting Information S1). These regions are the ones for which the ERA5-Land shows a better agreement with the other data sets in terms of the interannual variability of the seasonal maxima of daily maximum temperatures (Figure 1).

For each season, a heatwave is defined as "very extreme" when its corresponding HWMId value is larger than the 99.9th percentile of the values calculated for all the points of a given subdomain over the period 1950–1985.

3. Results

Prior to the comparison of the considered indices applied to daily temperature maxima derived from ERA5-Land, an evaluation of ERA5-Land against BE and JRA-55 is conducted in terms of the interannual variability of seasonal maxima of the target variable for each grid-cell of the domain. This allows us to better understand where the data are reliable for the estimation of the most intense heatwaves of a given period.

Figure 1 shows global maps of the Spearman rank correlation calculated over each grid point of the domain at a 1°longitude × 1°latitude spatial resolution, between the time-series of seasonal maxima of daily maximum
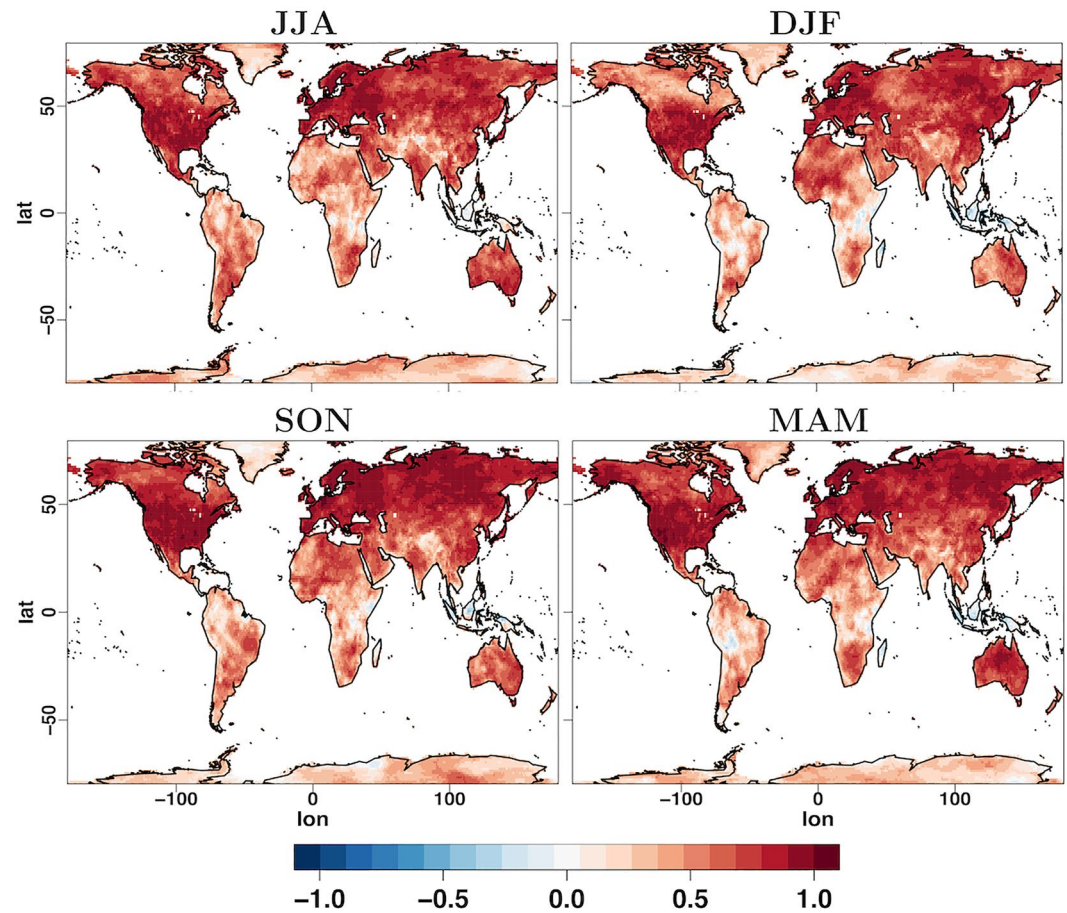
Figure 1. Spearman correlation calculated for the seasonal temperature maxima between ERA5-Land and Berkeley Earth, over the period 1950–2021, at 1 × 1°resolution. The correlation is calculated for each season separately (clockwise starting from the top-left corner: June July August, DJF, SON, and MAM).

temperatures derived from ERA5-Land and BE. In all seasons, the two data sets show a good agreement in terms of the considered variable between 30°N and 65°N, while the agreement between the data sets in the continental Southern Hemisphere is lower. For the tropical regions of South America and Africa, even negative correlations are evident in some cases between the two data sets. Regions characterized by complex topography, such as Greenland, Antarctica and the Tibetan plateau, also show very low correlation between ERA5-Land and BE, with values generally lower than +0.2 for all seasons. Northern North America exhibits low correlation (below +0.5) in DJF. Also, Western Australia shows a lower correlation in DJF and SON than in the other seasons. The same analyses conducted between ERA-Land and JRA-55 produce a slightly better agreement between the two data sets than between ERA5-Land and BE, even though large parts of the southern hemisphere still exhibit correlations below 0.5 in all seasons (Figure S2 in Supporting Information S1). This agrees well with the findings of Thompson et al. (2022), revealing a significant discrepancy between the two data sets over a large part of the continental Southern Hemisphere in terms of the most intense heatwaves of the period 1958–2021. A similar spatial agreement between the different data sets is also obtained when calculating the Spearman Rank correlation onto the JJA maxima of HWMId (Figure S3 in Supporting Information S1).

In a next step, daily maximum temperatures from the ERA5-Land data set at a spatial resolution of 0.25°longitude × 0.25°latitude are used to determine the most intense heatwaves of the period 1950–2021 and the year in which they occur, according to the four indices defined in Section 2.3. The goal is to investigate whether and how the detection of the most extreme events changes when considering definitions of heatwave intensity either based on cumulative or averaged values. Figure 2 shows the grid-cell maxima of the four given indices for JJA, over the period 1950–2021. Figure 2 illustrates how the AVI has a completely different pattern of the maxima with respect to the other indices. This is due to the fact that the AVI considers absolute temperatures: for this index it
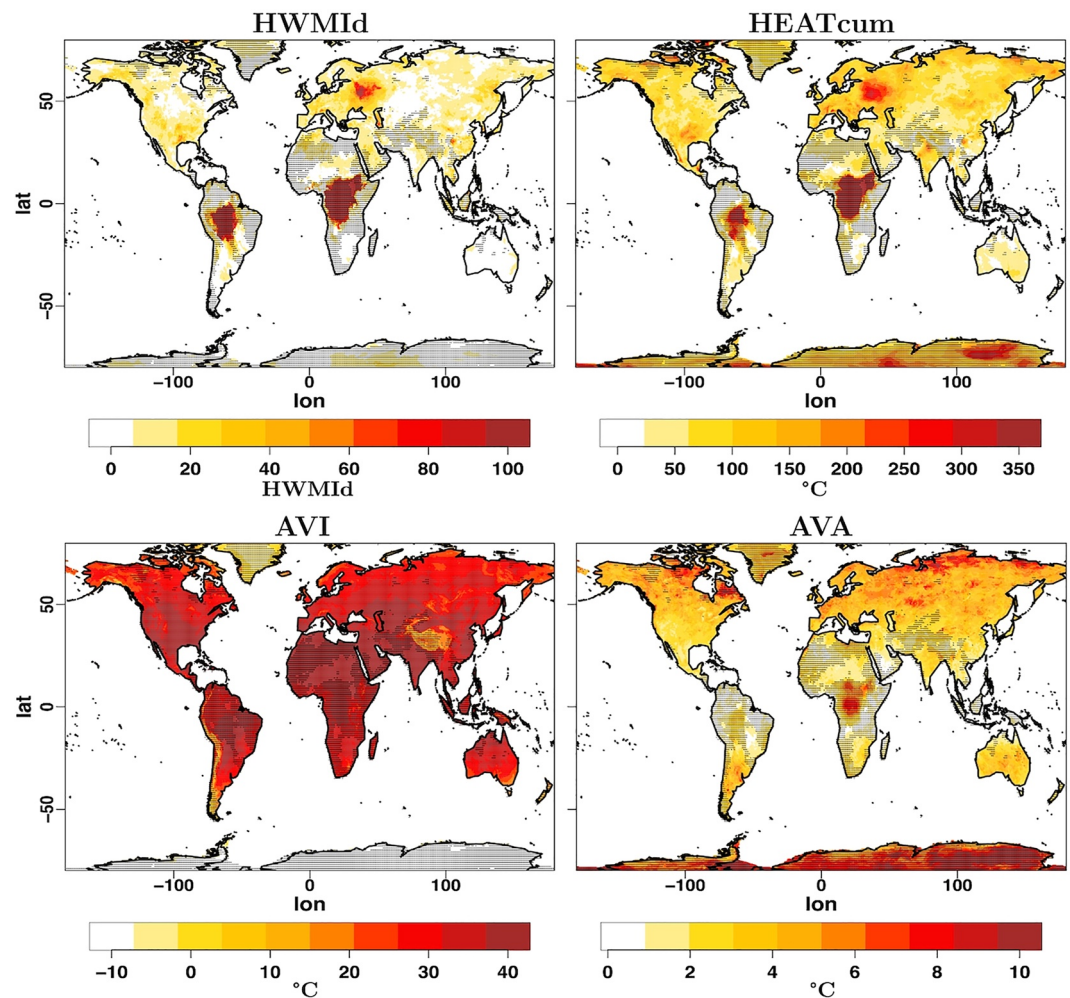
Figure 2. June July August maximum values of (clockwise starting from the top-left corner) HeatWave Magnitude Index daily, cumulative heat, Average Intensity, and AVA, applied to ERA5-Land daily maximum temperatures over the period 1950–2021. The grid-cells for which the correlation of seasonal maxima of daily maximum temperatures between ERA5-Land and BE is lower than +0.5 are shaded in gray.

is not possible to properly compare extremes over regions characterized by different climatologies. Considering the indices based on temperature anomalies, the AVA, relying on temporal averages, has a different pattern of the maxima with respect to the two other indices (i.e., HWMId and HEATcum). In particular, while HWMId and HEATcum both have some of their highest JJA values over Western Russia, which can be associated with the extreme summer heatwave of 2010 (Russo et al., 2014, 2015), values of AVA over this region are not very pronounced. This behavior is noticeable also when considering the extreme values of HWMId and HEATcum for Central Africa and South America (where ERA5-Land exhibits a strong disagreement with respect to the other data sets): these anomalous events almost disappear in the case of AVA, in all seasons (Figure S4 in Supporting Information S1).

Another interesting way to look at possible differences arising from the application of the different metrics is by considering, for each grid-cell, the years when the corresponding event with maximum intensity occurs over the period 1950–2021. Figure 3 shows that the maps of the year when the JJA maxima in the given metrics occur are pretty similar in the case of HWMId and HEATcum, presenting a spatial pattern correlation of ∼0.6. Conversely, the AVI and AVA show a very different spatial distribution compared to the two other metrics, with spatial correlations calculated against HEATcum of ∼0.2 in both cases. Importantly, the differences between AVA and HEATcum are considerably larger than the differences between HWMId and HEATcum, even though HWMId is based on a different target variable (i.e., standardized anomalies of daily temperature maxima) and considers
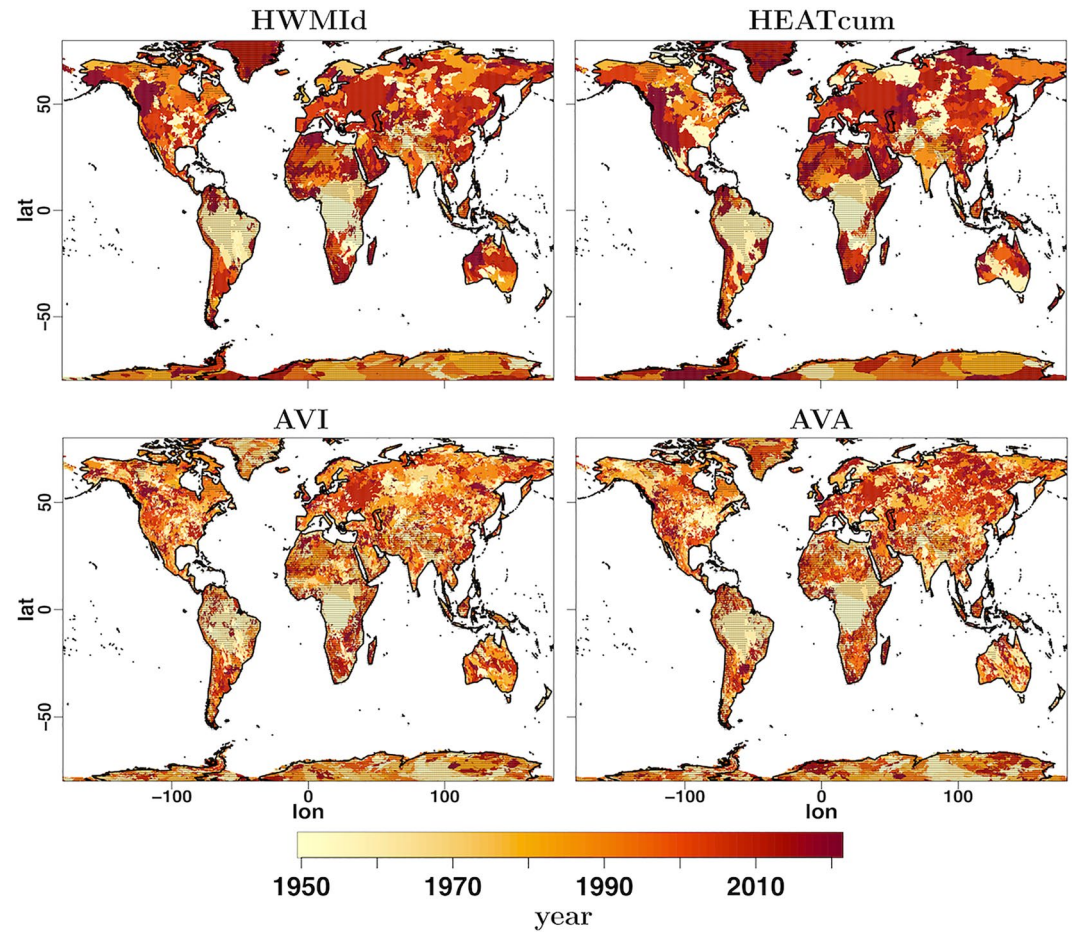
Figure 3. As in Figure 2, but for the year when the June July August maximum values of (clockwise starting from the top-left corner) HeatWave Magnitude Index daily, cumulative heat, Average Intensity, and AVA occur over the period 1950–2021, according to ERA5-Land daily maximum temperatures. The grid-cells for which the correlation of seasonal maxima of daily maximum temperatures between ERA5-Land and BE is lower than +0.5 are shaded in gray.

single heatwaves of a season. This is true also when considering other seasons (Figure S5 in Supporting Information S1), when calculating the HWMId over all the heatwave days of a season, as for HEATcum (Figure S6 in Supporting Information S1), as well as when conducting the same analysis on different data sets (Figures S7 and S8 in Supporting Information S1). Hence, the conclusions that can be drawn from the two groups of indices on the most intense events and the years in which they occur are substantially different.

Finally, the trends in the intensity of single heatwave events are investigated over the entire period 1950–2021. The HWMId allows us to calculate heatwave intensity for single events, while at the same time providing a standardized measure of extreme heat useful for the comparison across time and space. Hence, for the analysis of changes in very extreme events as defined in Section 2.4, the HWMId of single heatwaves over the period 1950–2021 is calculated for the three selected subregions CNA, EUR, and NAS (see Figure S1 in Supporting Information S1).

Figure 4 shows for each season and considered region the number of very extreme heatwaves for different values of HWMId. In general, a higher number and more intense extreme heatwaves are evident over the period 1986–2021 compared to 1950–1985, in all seasons and regions. In CNA, the maximum intensities are higher during LP than in EP, for all seasons, up to almost two times in DJF. The number of very extreme events also strongly increases in all seasons in this region during LP compared to EP, up to almost four times more in MAM. In CNA, only a small number of LP events present a value of HWMId higher than the maximum recorded in EP (vertical dotted line, Figure 4), up to 118 events more during JJA. In NAS, the maximum intensities are also more
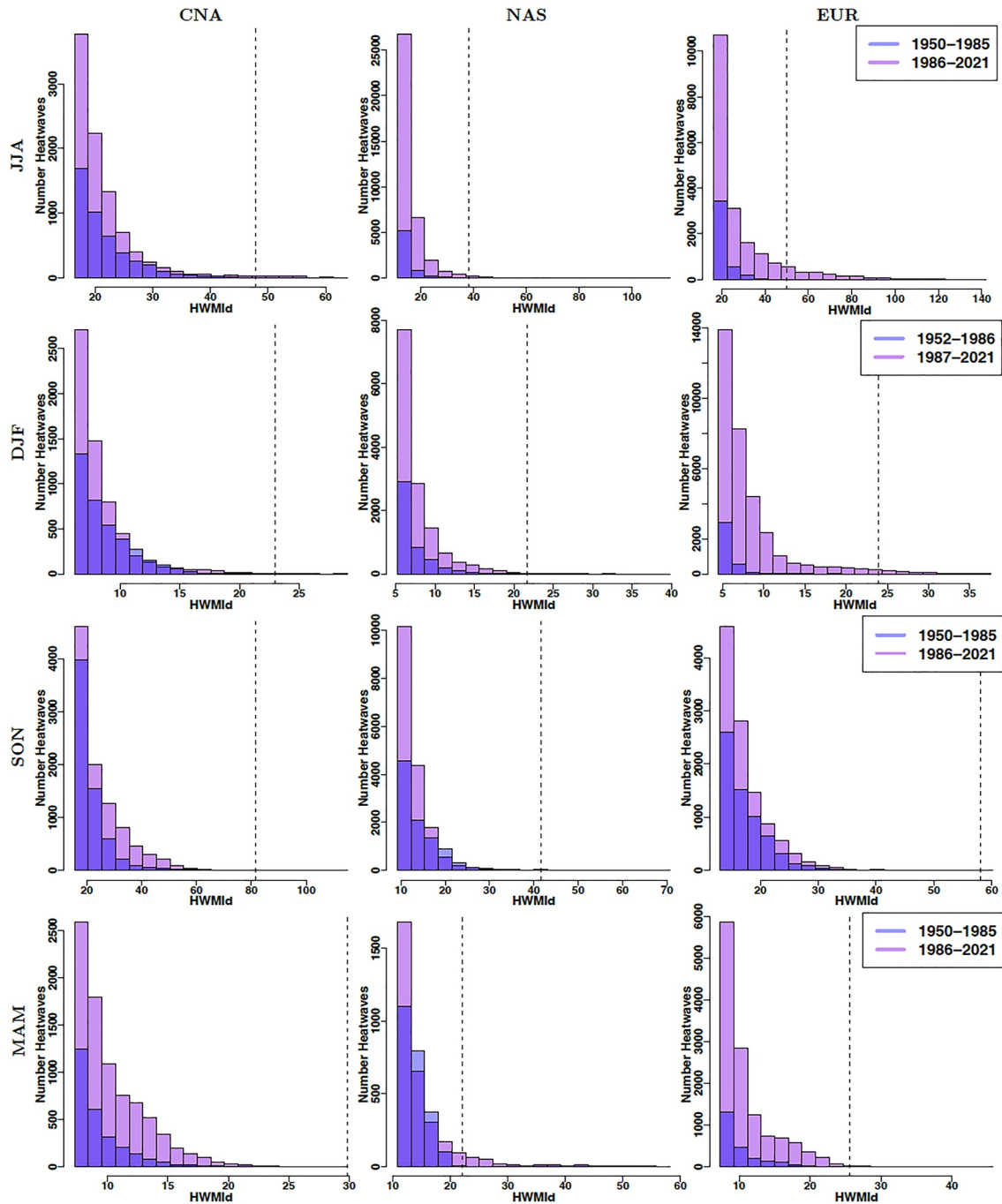
Figure 4. Number of heatwaves with intensities higher than the 99.9th percentile of HeatWave Magnitude Index daily (HWMId) calculated from ERA5-Land for each season of the period 1950–1985 and for all the grid-cells of Central North America, Northern Asia, and Northern Europe. From top to bottom, results for, respectively, June July August, DJF, SON, and MAM are represented through *light blue* bars for the period 1950–1985 and in *purple* for the period 1986–2021. The regions where the bars for both periods overlap are highlighted in darker purple. For each region and season the values of HWMId vary in between the corresponding 99.9th percentile of 1950–1985 and the maximum value of the entire period 1950–2021. The range of both HWMId and number of heatwaves changes amongst the different panels, since the number of grid points, events, as well as the value of the 99.9th percentile is different in each case. The dashed vertical line in each panel represents the maximum HWMId value recorded during 1950–1985 for the corresponding region and season.

pronounced during the most recent of the two periods, for all seasons, with values up to more than three times higher in JJA. For NAS the number of very extreme events increases by more than a factor of two over LP, in all seasons, with an exceptional increase by a factor greater than five in JJA. For the same region, during LP, a large amount of events presents HWMId values higher than the highest EP value, for a maximum of 259 times in JJA

and 300 in MAM. The largest changes between the two periods in both the number of events and their maximum intensities are evident for Europe, in particular in JJA, DJF, and MAM. Here an event considered very extreme during EP occurs at least four times more often during the most recent period in JJA and MAM, and more than nine times in DJF. The maximum HWMId value registered over the two periods for EUR is almost the same in SON and MAM, approximately twice in DJF and up to three times more in JJA during recent times. Additionally, for EUR, in an exceptionally high number of cases the maximum HWMId value of the period 1950–1985 is exceeded during the most recent period, up to 615 times in DJF and almost 2000 times in JJA.

4. Discussion and Conclusions

Several studies have called for a more unified definition and assessment of heatwave characteristics (Perkins & Alexander, 2013; Perkins-Kirkpatrick & Lewis, 2020). Nonetheless, in the climate and weather community, a plethora of different approaches is still employed for the definition of heatwave intensity, with metrics based on cumulative or averaged values of a target variable often used for referring to the same feature.

The results presented in this study show that the selection of metrics for the assessment of heatwave intensity needs caution: the year and spatial distribution of the most intense events over the period 1950–2021, as calculated from ERA5-Land daily maximum temperatures, change remarkably when considering two different families of metrics either relying on temporal averages or on cumulative values.

The use of heatwave intensity indices based on cumulative values should be preferred over the ones relying on temporal averages since, as already suggested by Russo et al. (2014), assessing intensity through averaged values does not allow for an unequivocal comparison of the magnitude of events with differing length. One simple example that could help in clarifying this point further is by considering two different heatwaves, the first one, HW1, lasting 3 days and the second, HW2, lasting 4 days. Let us suppose that HW1 has a value of the anomalies of +3°C for each of the three heatwave days, and HW2 has anomalies of +3°C for three heatwave days and of 2°C for the fourth one. When considering the average value of the anomalies, the event HW1 (mean value = +3°C) will misleadingly be considered more intense than HW2 (mean value = +2.75°C).

While measures of average heatwave intensity can be used for characterizing heatwaves, the comparison of events based on such metrics must be conducted with extreme care and is possible only when considering averaged intensity jointly with the length of an event. In climate and weather applications examining heatwaves in terms of departures from a reference value, a more unequivocal approach that could avoid any possible misleading assessment of heatwaves, allowing for a better comparison of events of different length, is to measure the intensity by cumulative values of the anomalies with respect to a given threshold. This choice is further justified by the fact that the impact of heatwaves is primarily determined by the accumulation of excess heat experienced over a specific time period, rather than relying on averaged values (Guo et al., 2017; Perkins-Kirkpatrick & Lewis, 2020). This measure can then be accompanied by the measurement of additional features such as the maximum amplitude of an event and its duration, following the framework proposed for hydro-climate extremes by Biondi et al. (2005, 2008) and Zuniga et al. (2021).

Based on these considerations, a grid-point-based analysis of the trends of heatwaves over the distinct periods 1950–1985 and 1986–2021 is successively performed using the cumulative index HWMId of Russo et al. (2015). In this case, only the regions where ERA5-Land presents a higher correlation against JRA-55 and BE in terms of the interannual variability of seasonal maxima of daily maximum temperatures are considered, namely Europe, CNA, and NAS. Overall, there is a clear increase in the number and intensity of heatwaves over the recent years 1986–2021, compared to what was considered very extreme during 1950–1985. Europe is the area where the most pronounced changes between the two periods emerge, with the total number of very extreme events increasing almost ten-fold in boreal winter, and the maximum intensity reaching values up to three times higher in boreal summer during the most recent times, compared to the former period: what was almost impossible during the period 1950–1985 has become more common and extreme during the years from 1986 to 2021.

This study sets the basis for a more unified and improved use of metrics for the calculation and comparison of heatwave intensity, at the same time providing an analysis of the trends in the number and intensity of very extreme events over the period from 1950 to 2021, for selected regions, revealing exceptionally severe changes in heatwaves.

Data Availability Statement

The ERA5-Land hourly near surface temperature data used for the computation of the different heatwave indices proposed in the study are available at the ECMWF Copernicus Climate Change Service (C3S) Climate Data Store (CDS) via https://doi.org/10.24381/cds.e2161bac. The Berkeley-Earth gridded daily maximum temperature observational data are available at http://berkeleyearth.org/data/. 6-hourly JRA-55 near-surface temperature data are available at the Research Data Archive of the National Center for Atmospheric Research, Computational and Information Systems Laboratory, via https://doi.org/10.5065/D6HH6H41. The scripts used for the performance of the presented analysis are available at the following link: https://doi.org/10.5281/zenodo.7974769.

References

Biondi, F., Kozubowski, T., & Panorska, A. (2005). A new model for quantifying climate episodes. *International Journal of Climatology: A Journal of the Royal Meteorological Society*, *25*(9), 1253–1264. https://doi.org/10.1002/joc.1186

Biondi, F., Kozubowski, T., Panorska, A., & Saito, L. (2008). A new stochastic model of episode peak and duration for eco-hydro-climatic applications. *Ecological Modelling*, *211*(3–4), 383–395. https://doi.org/10.1016/j.ecolmodel.2007.09.019

Bitencourt, D., Fuentes, M., Maia, P., & Amorim, F. (2016). Frequency, duration, spatial coverage, and intensity of heat waves in Brazil. *Revista Brasileira de Meteorologia*, *31*(4), 506–517. https://doi.org/10.1590/0102-778631231420150077

Breshears, D., Fontaine, J., Ruthrof, K., Field, J., Feng, X., Burger, J., et al. (2021). Underappreciated plant vulnerabilities to heat waves. *New Phytologist*, *231*(1), 32–39. https://doi.org/10.1111/nph.17348

Cowan, T., Purich, A., Perkins, S., Pezza, A., Boschat, G., & Sadler, K. (2014). More frequent, longer, and hotter heat waves for Australia in the twenty-first century. *Journal of Climate*, *27*(15), 5851–5871. https://doi.org/10.1175/jcli-d-14-00092.1

Cueto, R. G., Martínez, A., & Ostos, E. (2010). Heat waves and heat days in an arid city in the northwest of Mexico: Current trends and in climate change scenarios. *International Journal of Biometeorology*, *54*(4), 335–345. https://doi.org/10.1007/s00484-009-0283-7

Cusack, L., de Crespigny, C., & Athanasos, P. (2011). Heatwaves and their impact on people with alcohol, drug and mental health conditions: A discussion paper on clinical practice considerations. *Journal of Advanced Nursing*, *67*(4), 915–922. https://doi.org/10.1111/j.1365-2648.2010.05551.x

Data, C. (2009). *Guidelines on analysis of extremes in a changing climate in support of informed decisions for adaptation*. World Meteorological Organization.

Domeisen, D., Eltahir, E., Fischer, E., Knutti, R., Perkins-Kirkpatrick, S., Schär, C., et al. (2022). Prediction and projection of heatwaves. *Nature Reviews Earth & Environment*, *4*, 1–15. https://doi.org/10.1038/s43017-022-00371-z

Fischer, E., & Schär, C. (2010). Consistent geographical patterns of changes in high-impact European heatwaves. *Nature Geoscience*, *3*(6), 398–403. https://doi.org/10.1038/ngeo866

Forzieri, G., Bianchi, A., Silva, F., Herrera, M., Leblois, A., Lavalle, C., et al. (2018). Escalating impacts of climate extremes on critical infrastructures in Europe. *Global Environmental Change*, *48*, 97–107. https://doi.org/10.1016/j.gloenvcha.2017.11.007

Ganguly, A., Steinhaeuser, K., Erickson, D. J., III, Branstetter, M., Parish, E., Singh, N., et al. (2009). Higher trends but larger uncertainty and geographic variability in 21st century temperature and heat waves. *Proceedings of the National Academy of Sciences of the United States of America*, *106*(37), 15555–15559. https://doi.org/10.1073/pnas.0904495106

García-León, D., Casanueva, A., Standardi, G., Burgstall, A., Flouris, A., & Nybo, L. (2021). Current and projected regional economic impacts of heatwaves in Europe. *Nature Communications*, *12*(1), 1–10. https://doi.org/10.1038/s41467-021-26050-z

Gasparrini, A., Guo, Y., Hashizume, M., Kinney, P. L., Petkova, E. P., Lavigne, E., et al. (2015). Temporal variation in heat–mortality associations: A multicountry study. *Environmental Health Perspectives*, *123*(11), 1200–1207. https://doi.org/10.1289/ehp.1409070

Guo, Y., Gasparrini, A., Armstrong, B. G., Tawatsupa, B., Tobias, A., Lavigne, E., et al. (2017). Heat wave and mortality: A multicountry, multi-community study. *Environmental Health Perspectives*, *125*(8), 087006. https://doi.org/10.1289/ehp1026

Hersbach, H., Bell, B., Berrisford, P., Hirahara, S., Horányi, A., Muñoz-Sabater, J., et al. (2020). The ERA5 global reanalysis. *Quarterly Journal of the Royal Meteorological Society*, *146*(730), 1999–2049. https://doi.org/10.1002/qj.3803

Holbrook, N., Hernaman, V., Koshiba, S., Lako, J., Kajtar, J., Amosa, P., & Singh, A. (2022). Impacts of marine heatwaves on tropical western and central Pacific island nations and their communities. *Global and Planetary Change*, *208*, 103680. https://doi.org/10.1016/j.gloplacha.2021.103680

Iwasaki, A., & Noda, T. (2018). A framework for quantifying the relationship between intensity and severity of impact of disturbance across types of events and species. *Scientific Reports*, *8*(1), 1–7. https://doi.org/10.1038/s41598-017-19048-5

Kjellstrom, T., Lemke, B., & Otto, M. (2013). Mapping occupational heat exposure and effects in South-East Asia: Ongoing time trends 1980–2011 and future estimates to 2050. *Industrial Health*, *51*(1), 56–67. https://doi.org/10.2486/indhealth.2012-0174

Kobayashi, S., Ota, Y., Harada, Y., Ebita, A., Moriya, M., Onoda, H., et al. (2015). The JRA-55 reanalysis: General specifications and basic characteristics. *Journal of the Meteorological Society of Japan. Series II*, *93*(1), 5–48. https://doi.org/10.2151/jmsj.2015-001

Kovats, R., & Kristie, L. (2006). Heatwaves and public health in Europe. *The European Journal of Public Health*, *16*(6), 592–599. https://doi.org/10.1093/eurpub/ckl049

Lhotka, O., & Kyselý, J. (2015). Characterizing joint effects of spatial extent, temperature magnitude and duration of heat waves and cold spells over central Europe. *International Journal of Climatology*, *35*(7), 1232–1244. https://doi.org/10.1002/joc.4050

López-Bueno, J., Navas-Martín, M., Linares, C., Mirón, I., Luna, M., Sánchez-Martínez, G., et al. (2021). Analysis of the impact of heat waves on daily mortality in urban and rural areas in Madrid. *Environmental Research*, *195*, 110892. https://doi.org/10.1016/j.envres.2021.110892

Maggiotto, G., Miani, A., Rizzo, E., Castellone, M., & Piscitelli, P. (2021). Heat waves and adaptation strategies in a mediterranean urban context. *Environmental Research*, *197*, 111066. https://doi.org/10.1016/j.envres.2021.111066

Muñoz-Sabater, J., Dutra, E., Agustí-Panareda, A., Albergel, C., Arduini, G., Balsamo, G., et al. (2021). ERA5-land: A state-of-the-art global reanalysis dataset for land applications. *Earth System Science Data*, *13*(9), 4349–4383. https://doi.org/10.5194/essd-13-4349-2021

Perkins, S., & Alexander, L. (2013). On the measurement of heat waves. *Journal of Climate*, *26*(13), 4500–4517. https://doi.org/10.1175/jcli-d-12-00383.1

Perkins, S., Alexander, L., & Nairn, J. (2012). Increasing frequency, intensity and duration of observed global heatwaves and warm spells. *Geophysical Research Letters*, *39*(20), L20714. https://doi.org/10.1029/2012gl053361

Perkins-Kirkpatrick, S., & Lewis, S. (2020). Increasing trends in regional heatwaves. *Nature Communications*, *11*(1), 1–8. https://doi.org/10.1038/s41467-020-16970-7

Peters-Lidard, C., Blackburn, E., Liang, X., & Wood, E. (1998). The effect of soil thermal conductivity parameterization on surface energy fluxes and temperatures. *Journal of the Atmospheric Sciences*, *55*(7), 1209–1224. https://doi.org/10.1175/1520-0469(1998)055<1209:teostc>2.0.co;2

Rohde, R., Muller, R., Jacobsen, R., Perlmutter, S., Rosenfeld, A., Wurtele, J., et al. (2013). Berkeley Earth temperature averaging process, geoinfor. geostat.-an overview, 1, 2. *Geoinformatics Geostatistics An Overview*, *1*(2), 20–100.

Russo, S., Dosio, A., Graversen, R., Sillmann, J., Carrao, H., Dunbar, M., et al. (2014). Magnitude of extreme heat waves in present climate and their projection in a warming world. *Journal of Geophysical Research: Atmospheres*, *119*(22), 12–500. https://doi.org/10.1002/2014jd022098

Russo, S., Marchese, A. F., Sillmann, J., & Immé, G. (2016). When will unusual heat waves become normal in a warming Africa? *Environmental Research Letters*, *11*(5), 054016. https://doi.org/10.1088/1748-9326/11/5/054016

Russo, S., Sillmann, J., & Fischer, E. (2015). Top ten European heatwaves since 1950 and their occurrence in the coming decades. *Environmental Research Letters*, *10*(12), 124003. https://doi.org/10.1088/1748-9326/10/12/124003

Russo, S., & Sterl, A. (2011). Global changes in indices describing moderate temperature extremes from the daily output of a climate model. *Journal of Geophysical Research*, *116*(D3), D03104. https://doi.org/10.1029/2010jd014727

Schaeffer, A., & Roughan, M. (2017). Subsurface intensification of marine heatwaves off southeastern Australia: The role of stratification and local winds. *Geophysical Research Letters*, *44*(10), 5025–5033. https://doi.org/10.1002/2017gl073714

Siegle, M., Taylor, E., & O'Connor, M. (2018). Prior heat accumulation reduces survival during subsequent experimental heat waves. *Journal of Experimental Marine Biology and Ecology*, *501*, 109–117. https://doi.org/10.1016/j.jembe.2018.01.012

Stone, B., Jr., Mallen, E., Rajput, M., Gronlund, C., Broadbent, A., Krayenhoff, E., et al. (2021). Compound climate and infrastructure events: How electrical grid failure alters heat wave risk. *Environmental Science & Technology*, *55*(10), 6957–6964. https://doi.org/10.1021/acs.est.1c00024

Tavakol, A., Rahmani, V., & Harrington, J. (2020). Evaluation of hot temperature extremes and heat waves in the Mississippi River Basin. *Atmospheric Research*, *239*, 104907. https://doi.org/10.1016/j.atmosres.2020.104907

Thompson, V., Kennedy-Asser, A., Vosper, E., Lo, Y., Huntingford, C., Andrews, O., et al. (2022). The 2021 western North America heat wave among the most extreme events ever recorded globally. *Science Advances*, *8*(18), eabm6860. https://doi.org/10.1126/sciadv.abm6860

Ward, K., Lauf, S., Kleinschmit, B., & Endlicher, W. (2016). Heat waves and urban heat islands in Europe: A review of relevant drivers. *Science of the Total Environment*, *569*, 527–539. https://doi.org/10.1016/j.scitotenv.2016.06.119

Williams, S., Nitschke, M., Weinstein, P., Pisaniello, D., Parton, K., & Bi, P. (2012). The impact of summer temperatures and heatwaves on mortality and morbidity in Perth, Australia 1994–2008. *Environment International*, *40*, 33–38. https://doi.org/10.1016/j.envint.2011.11.011

Xia, Y., Li, Y., Guan, D., Tinoco, D., Xia, J., Yan, Z., et al. (2018). Assessment of the economic impacts of heat waves: A case study of Nanjing, China. *Journal of Cleaner Production*, *171*, 811–819. https://doi.org/10.1016/j.jclepro.2017.10.069

Yu, S., Yan, Z., Freychet, N., & Li, Z. (2020). Trends in summer heatwaves in central Asia from 1917 to 2016: Association with large-scale atmospheric circulation patterns. *International Journal of Climatology*, *40*(1), 115–127. https://doi.org/10.1002/joc.6197

Zhang, Z., Li, Y., Chen, F., Barlage, M., & Li, Z. (2020). Evaluation of convection-permitting WRF conus simulation on the relationship between soil moisture and heatwaves. *Climate Dynamics*, *55*(1), 235–252. https://doi.org/10.1007/s00382-018-4508-5

Zuniga, F., Kozubowski, T., & Panorska, A. (2021). A generalized linear model for multivariate events. *Journal of Computational and Applied Mathematics*, *398*, 113655. https://doi.org/10.1016/j.cam.2021.113655